INVESTIGATION OF COMPRESSION FAILURE IN BRICK MASONRY ASSEMBLIES MADE WITH SOFT BRICK

Conference Paper · September 2017

2 authors:

Mehar babu Ravula
Indian Institute of Technology Hyderabad
3 PUBLICATIONS   **1** CITATION

SEE PROFILE

Kolluru Subramaniam
Indian Institute of Technology Hyderabad
117 PUBLICATIONS   **1,300** CITATIONS

SEE PROFILE

Some of the authors of this publication are also working on these related projects:

Project   Damage Assesment of Concrete Elements using PZT Based Sensors View project

Project   structural health monitoring of concrete using piezo electric sensors View project

INVESTIGATION OF COMPRESSION FAILURE IN BRICK MASONRY ASSEMBLIES MADE WITH SOFT BRICK

Mehar Babu Ravula[1] and Kolluru V. L. Subramaniam [2]

(1) PhD Student, Department of Civil Engineering, IIT Hyderabad, India

(2) Professor, Department of Civil Engineering, IIT Hyderabad, India

Authors	E-Mail	Fax	Postal address
Mehar Babu Ravula	*ce11p1004@iith.ac.in*		*Room 310, Academic Block A, IIT Hyderabad, Kandi, Sangareddy, Telangana - 502285*
Kolluru V. L. Subramaniam	*kvls@iith.ac.in*		

Corresponding author for the paper: Mehar Babu Ravula

Presenter of the paper during the Conference: Mehar Babu Ravula

INVESTIGATION OF COMPRESSION FAILURE IN BRICK MASONRY ASSEMBLIES MADE WITH SOFT BRICK

Mehar Babu Ravula[1] and Kolluru V. L. Subramaniam [2]

(1) PhD Student, Department of Civil Engineering, IIT Hyderabad, <u>India</u>

(2) Professor, Department of Civil Engineering, IIT Hyderabad, India

Abstract

An experimental investigation of compressive failure in masonry made of soft clay bricks is presented. Damage evolution associated with the formation and propagation of vertical splitting cracks during the compressive load response of masonry assemblies in the stack bonded arrangement is evaluated. Full-field surface displacements during the compression load response of the masonry are obtained using digital image correlation (DIC). A clear evidence of the crack forming in the mortar and propagating into the brick is established. In mortar with lower strength than the brick unit, failure is produced by spalling associated with multiple vertical cracks, which result in loss of load bearing area. For mortar with a higher strength than the brick, cracking occurs when the level of compression is a significant proportion of the compressive strength of the brick. Failure is a result of global instability produced by the localized crushing of the brick.

Keywords: Masonry, Dilatancy, Failure, Mortar, Brick, Soft.

1.   INTRODUCTION

Masonry is a composite material, constructed using brick units and mortar. The composite response of the masonry is determined by the relative stiffness's of the two components and the interaction between the components at different stress levels. Typically most studies are on masonry consisting of stiffer bricks and relatively softer mortar, which is applicable to the case of hard-fired bricks or stone [McNary and Abrams 1985; Atkinson and Noland 1983; Drysdale et al. 1994]. However, the use of soft clay bricks coupled with steady improvements in cements, have resulted in mortars having higher stiffness and higher compressive strength than the bricks. In most of India, mortar has comparable or higher compressive strength than the brick [Dayaratnam (1987), Sarangapani et al. (2002)]. The relationship between constituent properties, the compressive stress-strain relationship and the compressive strength of masonry made with such bricks have been investigated [Deodhar 2000, Gumaste et al. 2006, Kaushik et al. 2007]. Most of these studies however did not explicitly study the failure in the masonry as it relates to the state of stress in the constituent materials.

In this paper, an experimental investigation of the compressive behavior of masonry assemblies made with soft clay fired brick are reported. Two different mortars, one with compressive strength higher than the brick strength and another with compressive strength lower than the strength of the brick unit are used in the experimental program. Masonry assemblies in the stack bonded arrangement are tested to evaluate the influence of the relative strength of mortar on the observed damage evolution and compressive failure. The stack bonded layout was used since

the stress field in the constituent materials is simpler to interpret, and the complexities arising from the head joint are avoided. Further, the stack bonded test configuration is also recommended in the codes of practice for evaluating the strength of masonry [IS 1905, SP20, ASTM C1314]. In the test program, the evolution of damage in the brick and the mortar is investigated using the surface displacements measured using the DIC technique.

Background

The compressive strength of masonry depends on characteristics of the brick unit and the mortar. During compression of masonry prisms with stiff bricks and soft mortar, the mortar is in a state of triaxial compression and the brick is subjected to in-plane biaxial tension coupled with axial compression. This state of stress results in vertical splitting cracks in bricks, which ultimately leads to the failure of the masonry prisms [McNary and Abrams 1985; Atkinson and Noland 1983; Drysdale et al. 1994].

Very few investigations on the compressive behavior of low-strength clay brick masonry have been reported in the literature [Matthana (1996), Sarangapani et al. (2005), Raghunath and Jagadish (1998) and Gumaste et al. (2004)]. In masonry made of low strength brick, the compressive strength of the masonry strength is lower than the compressive strengths of both the brick unit and the mortar [Kaushik et al. (2007), Sarangapani et al. (2007), Gumaste et al. (2007)]. Typically, low strength bricks have lower elastic modulus than the mortar. For an applied axial stress on the masonry, a triaxial compression state of stress is produced in the bricks while the mortar joints are under a biaxial tension stress state with superimposed axial compression. (shown in Figure 1). The major form of distress in the masonry is associated with splitting of bricks, which ultimately produces failure [Gumaste et al. (2007), Reddy and Vyas (2008), Kaushik et al. (2007)]. An understanding of the failure in masonry as it relates to the stress state resulting from composite material behavior of brick units and mortar is still not available.
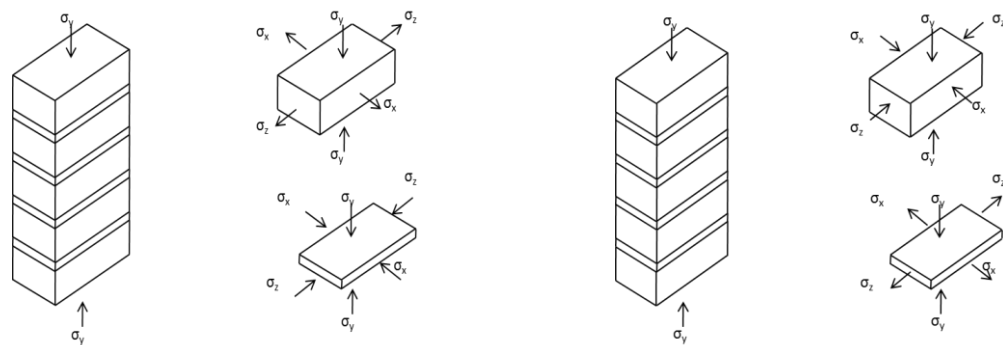

Figure 1: Stress states in masonry under compression for (a) stiff brick (b) soft brick.

2.   EXPERIMENTAL PROGRAM

In the experimental program, the compressive response of wire cut bricks, mortar and stack bonded masonry was evaluated. Extruded, wire cut bricks were used in this study. The nominal dimensions of the bricks are 220 mm (length), 70 mm (height) and 100 mm (thickness). The water absorption of the bricks determined as per the requirements of IS 3495(part2):1992 was 9 percent.

In the study, two different mortar compositions given by volumetric proportions of cement: sand equal to 1:3 and 1:6 were used. The mortar with cement:sand equal

to 1:3/1:6 is referred to as the strong/weak mortar. Mortar cylinders of 100 mm diameter and height equal to 200 mm were prepared from the same mortar mix used for preparing masonry specimens. Specimens were covered with a wet burlap immediately after casting. The specimens were demoulded after one day and kept in curing tank for 28 days.

Stack bonded masonry specimens consisting of five bricks and four mortar joints were prepared. Following the procedure reported by Sarangapani et al. (2005), the brick units used in preparing the masonry assemblage were first submerged in water for two hours before laying, to allow better brick-mortar bond development. After casting, the masonry specimens were kept wrapped in a moist burlap up to testing.

3.   COMPRESSIVE BEHAVIOR OF BRICK

Compression tests were performed on brick blocks with cross-sectional dimensions equal to 35 mm x 35 mm and height equal to 70 mm, which were cut from the brick unit. The top and bottom square cross-sectional surfaces of the specimens were capped with a thin layer of plaster-of-Paris (gypsum plaster) to provide a uniform, level contact surface with the platens of the test machine. Initially, the load was cycled and the deformation over a gage length of 35 mm was measured using a surface mounted clip gage. After load cycles, the clip gage was removed and the specimens were tested in load control, up to failure. The Young's modulus measured from the brick blocks using the surface mounted gage was 1.09 GPa (standard deviation of 230 MPa). The compressive strength obtained from blocks was 7.4 MPa (coefficient of variation 0.16).

The compressive stress-strain response of the entire brick unit was obtained from a displacement controlled test. The deformation of the brick was recorded using a pair surface mounted linear variable displacement transformers (LVDT) mounted on opposite faces of the brick over a gage length of 35 mm. Additionally, the lateral expansion of the brick was measured using two LVDTs which were reacted off of the brick at the mid-height location. During the test, the rate of displacement measured between the two platens was increased at the rate of 0.6 mm per minute. Typical stress-strain response of the brick unit is shown in Figure 2(a). The lateral expansion of the brick is also plotted in the figure for comparison. A photograph of the failed specimen of the brick unit is shown in Figure 2(b). The failure of the specimen was observed to be produced by vertical cracks. The cracks were observed to form in the pre-peak part of the load response associated with the onset of significant non-linear response. In the non-linear pre-peak load response, the formation of the vertical cracks contributed to the increase in the lateral strain. The crack opening displacement produced by cracks, resulted in very large values of lateral strain. Calculation of continuum measure of Poisson's ratio is therefore misleading after the formation of the vertical cracks. The average compressive strength obtained from ten brick units was 13.98 MPa (coefficient of variation was equal to 0.178). The Poisson's ratio of the bricks determined in the early part of the load response was 0.25 (standard deviation was 0.15).

The compressive strength obtained from the brick unit is significantly higher than the strength obtained from blocks of smaller size cut from the brick. This suggests the influence of end constraints from platens [Morel et. al. (2007)]. Both specimens had the same height but different cross-sectional areas. The compressive response obtained from blocks cut from the brick units are representative of the unconfined behavior of the material. There is a significant influence of self-

confinement on the compressive response obtained from the brick unit. Under an applied compression, the level of confinement would be the highest at the geometric center of the brick unit. Considering the confinement of the material, higher compressive strength is obtained from the brick unit. The unconfined compressive strength of the material obtained from the brick block is smaller than the strength of the brick unit. This factor is acknowledged in Eurocode for structural masonry and block strengths are normalized by applying an empirically derived shape factor to account for aspect ratio effects [EN 1996-1-1:2003, Krefeld (1983)]. The aspect ratio (height/least width) for the brick unit is 2.0, and the correction factors for obtaining the unconfined compressive strength from the compressive strengths of the brick unit is 0.6. The unconfined compressive strength of the brick predicted using the correction factor is equal to 8.4 MPa, which is close, but higher than the value obtained from the blocks.
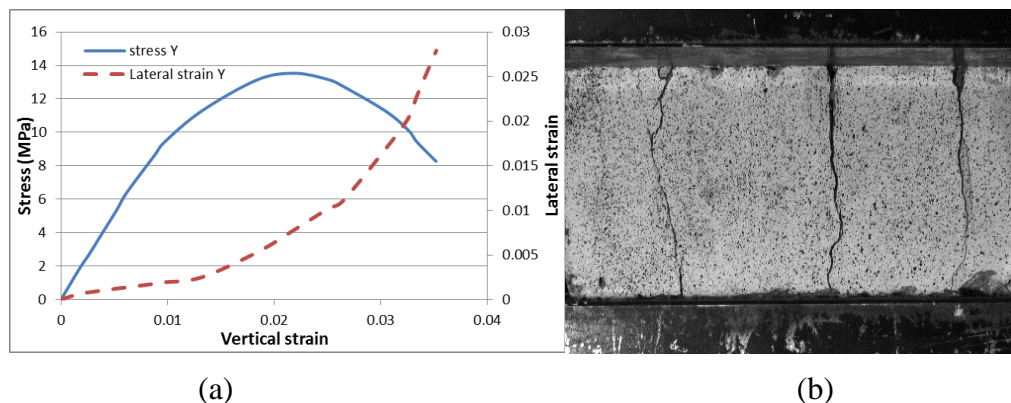

(a) (b)

Figure 2: (a) Stress-strain response of brick unit tested in compression; (b) Typical failed specimen of brick unit.

4.   COMPRESSIVE BEHAVIOR OF MORTAR

Mortar cylinder specimens were capped using a capping compound prior to testing. The axial deformation of the specimen was recorded using LVDTs attached to surface mounted rings over a gage length of 60 mm. The lateral expansion of the specimen was recorded using two LVDTs which were reacted off of the specimen at the mid-height location. During the test, the rate of displacement measured between the two platens was increased at the rate of 0.6 mm per minute. Typical stress-strain behaviour of mortar specimens is shown in Figures 3 (a) and (b) for the weak and the strong mortars, respectively. The onset of non-linearity in the compressive response is associated with an increase in the rate of lateral expansion. Comparing the two mortars, it can be seen that there is a significantly larger lateral strain at peak load in the weak mortar when compared with the strong mortar. This corresponds with the larger extent of cracking observed in the weak mortar when compared with the strong mortar. Significant dilatancy is observed in the post-peak part of the load response, where there is significant increase in the lateral strain. A comparison of the stress-strain curves of the two mortars are plotted on non-dimensional axes in Figure 3(c). The values of stress have been normalized with respect to the peak stress and the values of strain have been normalized with respect to the strain corresponding to the peak. The pre-peak responses of the strong and weak mortars are nominally similar. The strong mortar however exhibits a more brittle post-peak response. The results from the mortar are summarized in Table 1.
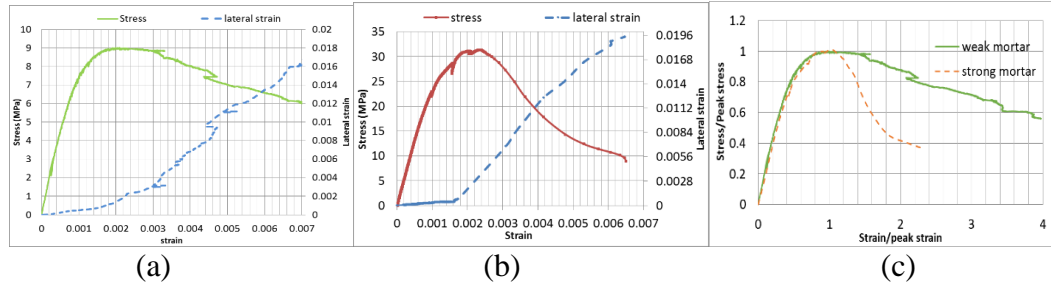
Figure 3: Stress-strain response of mortar (a) weak mortar; (b) strong mortar; and (c) compression responses of strong and weak mortars in a non-dimensional plot.

5.   COMPRESSIVE BEHAVIOR OF MASONRY

The top and bottom surfaces of the masonry specimens were capped with a thin layer of Gypsum to ensure uniform contact with the platens of the test machine. The front face of the masonry specimen was prepared for digital image correlation by creating a sprayed-on speckle pattern [Ravula and Subramaniam (2017)]. Local measurement of vertical strains are obtained from the average of two LVDTs fixed on the side surfaces between the 2nd brick and 4th over a gauge length of 160 mm. In a typical compression test, the rate of displacement measured between the two platens of the test machine were increased at a constant rate of 0.6 mm/minute. During the compression test, images of the specimen were captured for correlation using a high resolution camera (5 mega pixel). The camera was fitted with a 50 mm lens and was placed at a distance of 1 m from the specimen surface. Uniform light intensity was ensured across the surface of the masonry using normal white light. A schematic diagram of the test setup is shown in Figure 5. A reference image was captured in the undeformed state prior to the initiation of loading program.

The typical stress-strain curves obtained from the surface mounted LVDTs are shown in Figures 4(a) and 4(b) for the specimens made with the weak and the strong mortars, respectively. Specimens made with both mortars exhibited strengths which are lower than the compressive strengths of both the constituent materials. The results of the mechanical characteristics masonry are summarized in Table 1.

Table 1: Characteristics of mortar and masonry

Material	Specimen size mm	Strength (Std. Dev.) MPa	E (Std. Dev.) GPa	Peak strain (Std. Dev.)
Strong Mortar	100 mm cylinder	30 (1.75)	26.5 (0.442)	0.0025 (0.00043)
Weak Mortar	100 mm cylinder	9.36 (1.77)	8.0 (0.176)	0.00203 0.00024)
Masonry with strong mortar	220 ×100×380 (l x b x h)	7.95 (0.2)	0.96 (0.056)	0.0083 0.00084)
Masonry with weak mortar	220 ×100×380 (l x b x h)	5.8 (0.34)	0.88 0.041)	0.0082 (0.0015)

While the peak loads are not significantly different, there are considerable differences in the load responses and modes of failure in the masonry specimens made from the two mortars. Specimens with the weak mortar exhibit a significantly higher level of pre-peak non-linearity. The response of specimens made with the strong mortar exhibit an almost linear response up to the peak load. The failure of specimens with the strong mortar was significantly more brittle with a very rapid decrease in load in the post-peak.

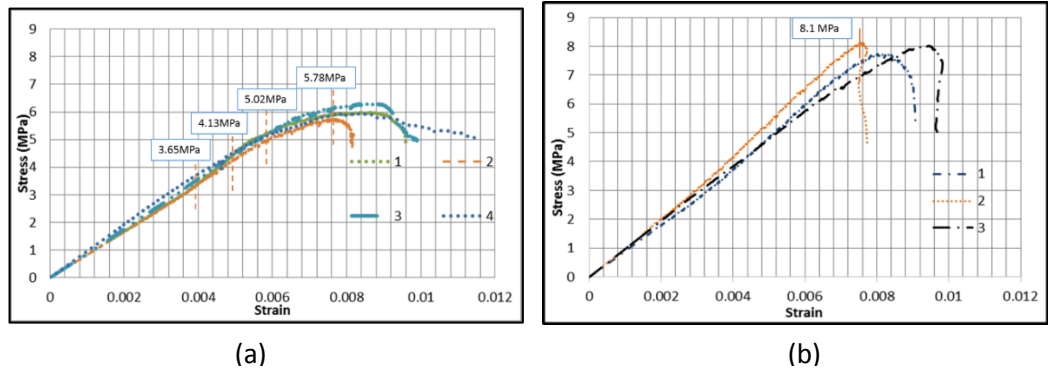(a)   (b)

Figure 4: Load response of the stack bonded masonry prism with (a) weak mortar and (b) strong mortar.
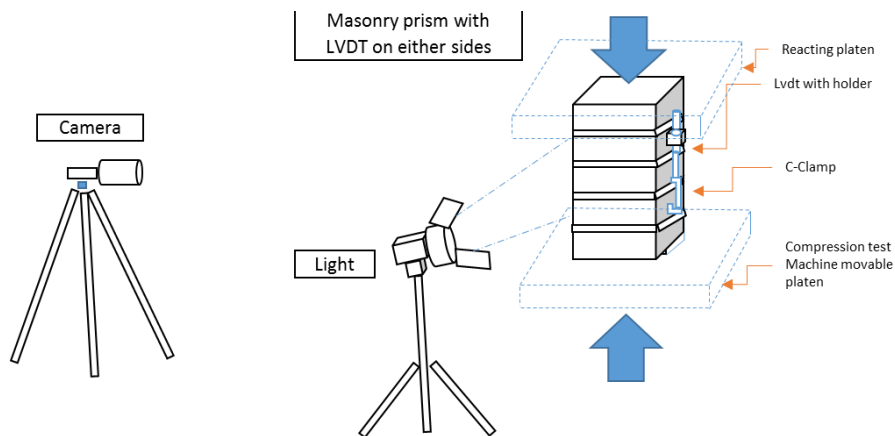

Figure 5 : Schematic test setup for masonry prism test

6.   ANALYSIS OF COMPRESSION RESPONSE

A two-dimensional displacement field on the surface of the masonry specimen was obtained from cross-correlation of images the undeformed specimen with the image in the deformed state [Sutton et al. (1983, 1988)]. A subset size equal to 32x32 pixels was used for the correlation. A Quintic B-spline interpolation of the grey values was used to achieve sub-pixel accuracy. The cross correlation analysis of the digital images was performed using the VIC-2D^{TM} software, which maximizes the correlation coefficient between grey levels in the subsets in the reference and deformed images. Surface displacements and displacement gradients at each loading stage were calculated at each subset center, by evaluating the shape functions and their partial derivatives at the subset center. For the setup used in this study, the random error in the measured displacement is in the range of 0.002 pixels. Strains were computed from the gradients of the displacements. A conservative

estimate of the resolution in strain obtained from the digital correlation was 10 $\mu\varepsilon$ [Bruck et al (1989), Schreier (2002)].

In masonry specimen with weak mortar, the crack initiation from the brick-mortar interface is shown in Figure 6(a). The load point at crack initiation is shown marked on the load response of the specimen in Figure 4(a). The formation of the crack coincides with the onset of non-linearity in the load response at an applied axial stress of 4.13MPa. The sharp profile of the crack is identified by closed contours with very high strain gradient in a small region. The displacement contours coalesce at the crack. On increasing the axial stress, the vertical splitting crack increased in length and the crack opening at the brick-mortar interface continued to increase. Subsequently, additional cracks were formed across the width of the specimens. Cracks in the specimen at an applied axial stress equal to 5.78 MPa are shown in Figure 6(b), where ε_{xx} is plotted over an area spanning three bricks and including two mortar joints. The corresponding ε_{yy} are plotted in Figure 6(c). Tensile splitting of the brick is driven by the differential lateral expansion of the brick and mortar at the interface, which results in the crack being the widest at the brick-mortar interface. In the contour plots of ε_{yy}, some strain localization is evident at the interface between brick and mortar at these load levels. Very high strains occur in a small region located at the interface. The local strains in compression in the interface region indicates some localized crushing in the material. The splitting cracks are initiated at different locations along different brick-mortar interfaces. These cracks eventually grow vertically across multiple joints. Failure occurred when several cracks joined causing spalling of a piece of the masonry reducing the load carrying area.
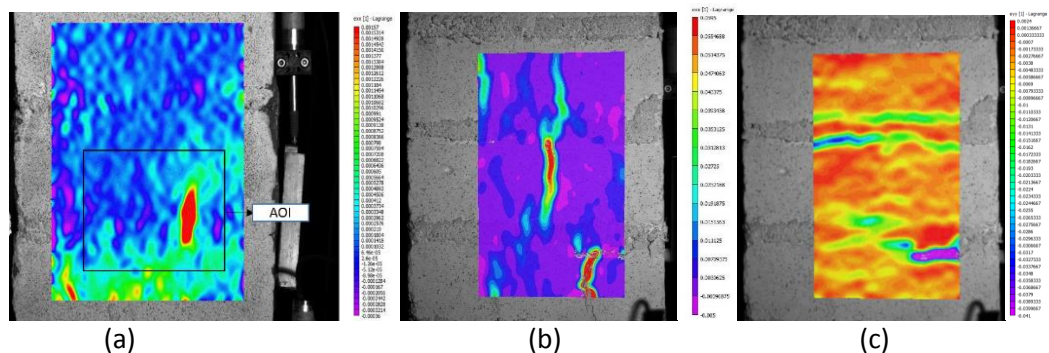

(a)   (b)   (c)

Figure 6 (a) Contour plot of ε_{xx} over the surface of the masonry specimen with weak mortar at applied axial stress equal to 4.13 MPa; (b) Contours of ε_{xx} at applied axial stress equal to 5.78 MPa (b) Contours of ε_{yy} at applied axial stress equal to 5.78 MPa

In masonry specimen made with the strong mortar, cracking was observed at a higher load level when compared with the masonry made with weak mortar. As the strong mortar tensile strength is higher compared with the weak mortar, cracking occurs later in the load response. The strain contours in the masonry specimen at an applied compressive stress equal to 8.1 MPa (shown marked on the load response in Figure 4) are shown in Figure 7. From the strain contours of ε_{xx} in Figure 7(b), the crack can be identified as starting from the mortar and it propagates into the brick. The corresponding vertical strain in the specimen is shown in Figure 7(c). Significant strain localization in ε_{yy} occurs in the brick-mortar interface region. Therefore while the global strain in the brick is not high, the localization increases

the magnitude of strain in a small region. The localization is likely attributed to the large difference in stiffness of brick and mortar. The brick is much softer compared to the mortar and hence cause axial strain accumulation at interface. The formation of the crack in the brick leads to a release of stress and loss of confinement from the mortar. The failure strength therefore approaches to that of unconfined brick strength. The ultimate failure was produced by global instability caused by the localized crushing and spalling of material from a small region.

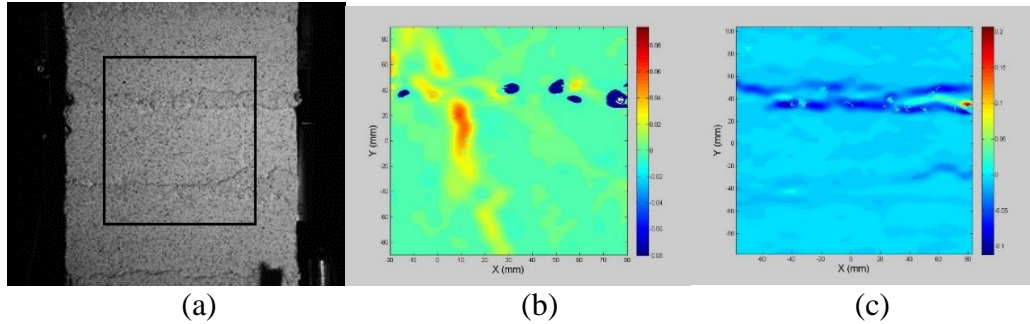| (a) | (b) | (c) |

Figure 7: Strain contour plot at mortar joint in prism specimen with 1:3 mortar at axial compressive stress equal to 8.1 MPa: (a) Area Of Interest used for correlation; (b) ε_{xx} contour showing crack initiation from the mortar joint; c) ε_{yy} contour showing strain localization at the mortar brick interface.

CONCLUSIONS

The results of the experimental program indicate that the compressive strength of the masonry made with soft brick is lower than the compressive strength of both brick and mortar irrespective of mortar strength. For a large increase in mortar strength, a small increase in masonry strength will be obtained. Compressive strength of masonry is insensitive to the mortar strength but the failure mode is directly influenced by the mortar strength relative to that of brick. For soft bricks, where the elastic modulus of brick is lower than the elastic modulus of the mortar, failure in both low and high-strength mortars is associated with cracking in bricks, which is initiated in the mortar.

Failure in low strength mortar is produced by spalling associated with vertical cracking in bricks. Failure in masonry with high-strength mortar is more brittle and is produced by localized crushing of bricks near the brick-mortar interface. Severe localized crushing of brick close to the interface at a value of stress close to the unconfined compressive strength of the brick material is produced. Failure is produced by the local crushing of the material leading to global instability

REFERENCES

1. McNary WS, Abrams DP (1985) Mechanics of masonry in compression. J Struct Eng 111(4):857–870
2. Atkinson RH and Noland JL. (1983) A proposed failure theory for brick masonry in compression. Proc., 3rd Canadian Masonry Symp., Edmonton, pp5.1–5.17.
3. Drysdale RG, Hamid AA., and Baker LR. (1994) Masonry structures: Behaviour and design. Prentice-Hall, Englewood Cliffs NJ.
4. Dayaratnam P (1987) Brick and reinforced brick structures. Oxford and IBH, New Delhi, India.

5. Sarangapani G, Venkatarama Reddy BV, and Jagadish KS (2002) Structural characteristics of bricks, mortar and masonry. J. Struct. Eng. (India), 29(2), 101–107.
6. Deodhar SV. (2000) Strength of Brick Masonry Prisms in Compression. J Institution of Eng (India), 81(3):133-137.
7. Gumaste KS, Venkatarama Reddy BV, Nanjunda Rao KS, Jagadish KS (2004) Properties of burnt bricks and mortars in India. Masonry Int 17(2):45–52.
8. Kaushik HB, Rai Durgesh C, Jain Sudhir K (2007) Stress-strain characteristics of clay brick masonry under uniaxial compression. J of Mater Civil Eng, 19(9):728-739.
9. IS 1905-1987 Code of practice for structural use of unreinforced masonry. Bureau of Indian Standard, New Delhi.
10. SP20 (1991) Handbook on masonry design and construction. Bureau of Indian standard.
11. ASTM (2003) Standard test method for compressive strength of masonry prisms. C1314-03b, ASTM International, West Conshohocken
12. Matthana MHS (1996) Strength of brick masonry and masonry walls with openings. Ph.D thesis, Department of Civil Engineering, Indian Institute of Science, Bangalore, India.
13. Sarangapani G, Venkatarama Reddy BV, Jagadish KS (2005) Brick–mortar bond and masonry compressive strength. J Mater Civil Eng (ASCE), 17(2):229–237.
14. Raghunath S, Jagadish KS (1998) Strength and elasticity of bricks in India. Workshop on Recent Advances in Masonry Construction, WRAMC-98, Roorkee, pp 141–150.
15. Gumaste KS, Rao KSN, Reddy BVV, Jagadish KS (2007) Strength and elasticity of brick masonry prisms and wallettes under compression. Mater and Struct 40:241–253.
16. Venkatarama Reddy BV, Uday Vyas ChV (2008) Influence of shear bond strength on compressive strength and stress–strain characteristics of masonry. Mater Struct 41:1697–1712.
17. IS3495 Part-2 (1992) Code of practice for Methods of test of burnt clay building bricks. Bureau of Indian Standard, New Delhi, India.
18. Morel JC, Pkla A, Walker P (2007) Compressive strength testing of compressed earth blocks. Constr and Building mater, 21(2):303-309.
19. CEN (2005) Eurocode 6-design of masonry structures Part 1-1: general rules for reinforced and unreinforced masonry structures. European Committee for Standardization, Brussels, Belgium.
20. Krefeld WJ. (1983) Effect of shape of specimen on the apparent compressive strength of brick masonry. Proceedings of American Society of Materials, 363-369.
21. Ravula MB, and Subramaniam KVL (2017) Experimental Investigation of compressive failure in masonry brick assemblages made with soft brick. Mater Struct, 50:19. Doi: 10.1617/s11527-016-0926-1.
22. Sutton MA, Wolters WJ, Peters WH, Ranson WF and McNeil SR (1983) Determination of displacements using an improved digital correlation method. Image and Vision Comput 1(3): 133-139.
23. Sutton MA, McNeill SR, Jang J. and Babai M (1988) Effects of sub-pixel image restoration on digital correlation error. J Opt Eng, 27(10):870-877.
24. Bruck HA, McNeil SR, Sutton MA and Peters WH (1989) Digital image correlation using newton-raphson method of partial differential correction. Exp Mech 29(3):261-267.
25. Schreier HW, Garcia D, Sutton MA (2002) Systematic errors in digital image correlation due to under-matched subset shape functions. Exp Mech 42(3):303-310.